

Spectroscopic studies of iron sulfide formation and phase relations at low temperatures

ALISTAIR R. LENNIE and DAVID J. VAUGHAN

Department of Earth Sciences, The University of Manchester, Oxford Road, Manchester M13 9PL, England

Abstract—The iron monosulfides mackinawite (Fe_{1+x}S) and “amorphous FeS ,” the first formed iron sulfides in aqueous systems at low temperatures, have been studied using X-ray photoelectron and X-ray absorption spectroscopies. The divalent oxidation state of Fe and the local structure environment of Fe and S in mackinawite have been confirmed. Comparisons of the Fe K-edge X-ray absorption spectra of synthetic mackinawite with those of “amorphous FeS ” precipitates subjected to ageing for periods ranging from 1 to 1800 seconds, and precipitated under pH conditions between pH 3.9 and pH 7.4, show the precipitates to have local structure consistent with that found in crystalline mackinawite. Combining these data with results in the literature leads to the proposal of a model which accounts for the formation from aqueous solution of Cubic FeS , troilite, and mackinawite. We use this model, which takes account of the effect of electron withdrawal by H^+ at the crystal surface, to propose that these three phases can all be formed from Fe in tetrahedral coordination with S. This model facilitates understanding of the phase relationships in the Fe-S system at low temperatures, whereby initial formation is of iron “monosulfides” with either cubic close-packed (ccp) or hexagonal close-packed (hcp) S sublattices. Subsequent sulfidation of either sublattice type will form pyrite (or marcasite). However, the predominant sulfidation sequence at low temperatures is:

[Cubic FeS]/amorphous $\text{FeS} \rightarrow$ mackinawite \rightarrow greigite \rightarrow marcasite/pyrite. Both the nucleation of hcp S sub-lattice phases in low temperature aqueous iron sulfide systems, and the formation of hcp phases by transformation from the cubic monosulfides, are inhibited by kinetic factors.

INTRODUCTION

THE MINERALS of the iron-sulfur system are important Earth and planetary materials for a number of reasons. Troilite (FeS) is an important phase in iron meteorites, suggesting that sulfur may coexist with iron in the core of the Earth. Iron sulfides, as well as occurring as accessory minerals in many common rocks, are major phases in the sulfide ore deposits that are still the main suppliers of many base (Cu, Pb, Zn), ferroalloy (Ni, Co, Mn), and rare or precious (Ga, Ge, Ag, Pt) metals. Studies of iron sulfide formation in Recent sediments via sulfate-reducing-bacteria, and in hydrothermal systems presently active at or near mid-ocean ridges, have stimulated new ideas regarding the role of sulfides in the geochemical cycling of the elements. These studies have not only furthered understanding of the processes of formation of metal sulfide ore deposits, but have also suggested that metal sulfides may entrap heavy metal pollutants in sediments. Furthermore, the discovery of life forms adapted to the warm but anoxic environments of sea-floor hydrothermal systems, and the known sulfur-metabolizing ancient bacteria, has fueled a debate that anoxic sulfide environments could have been the sites for the emergence of life on Earth. This debate has centred around iron sulfides which may have played a central role in supplying energy

and, perhaps, in catalysing reactions leading to the build-up of complex organic molecules.

At temperatures in excess of $\sim 350^\circ\text{C}$, the phase relations in the Fe-S system are relatively straightforward, but at lower temperatures the Fe-S system becomes much more complex and less well understood. In part, this arises from ordering of vacancies upon cooling of the pyrrhotite (Fe_{1-x}S) solid solution, forming complex superstructures. A further complexity concerns phases found only in relatively low temperature environments in nature, which can be synthesized only in solution. For this reason, these lower temperature phases may not even appear in the (equilibrium) phase diagrams that have generally been constructed on the basis of experiments involving reaction between elemental iron and sulfur in sealed evacuated silica capsules. Several important phases (notably marcasite, FeS_2 , and mackinawite Fe_{1+x}S) are of this type, along with a number of rarer minerals (greigite Fe_3S_4 and, possibly, smythite $\sim\text{Fe}_9\text{S}_{11}$) and phases so far found only in synthesis experiments (e.g., Cubic FeS). It seems very likely that all of these phases are metastable; indeed calculations of the free energies of formation of these phases confirm this view (see Fig. 1). Although some of these minerals appear to be rare in their geological occurrence, they are of considerable importance as transient species produced when iron and sulfur react in aqueous solutions, subsequently transforming to the more stable

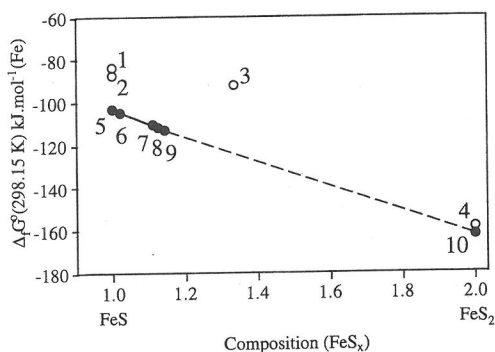


FIG. 1. Schematic free energy-composition diagram for the iron sulfide minerals. The gain in free energy, $\Delta_f G^\circ(298.15 \text{ K})$, in kJ.mol^{-1} (of Fe), is that obtained from forming the various sulfides from the elements. Open circles represent Amorphous FeS (1), mackinawite (2), greigite (3) and marcasite (4). Filled circles represent the pyrrhotites: Troilite (5), $\text{Fe}_{11}\text{S}_{12}$ (6), $\text{Fe}_{10}\text{S}_{11}$ (7), Fe_9S_{10} (8), Fe_7S_8 (9), and pyrite (10). Data for 1 - 3 are calculated from solubility data of DAVISON (1991); for 4 and 10 from CHASE *et al.* (1985) and for 5 - 9 from GRØNVOLD and STØLEN (1992). The dashed line is the join between monoclinic pyrrhotite and pyrite; the solid line is the join between troilite and monoclinic pyrrhotite. Free energy values for phases 1, 2, 3, and 4 lie above these lines suggesting metastability for these phases at this temperature.

phases (BONEV *et al.*, 1989). The keys to understanding these phases are concerned with their mechanisms of formation in solution, and with relationships to other iron sulfides, as determined by the kinetics and mechanisms of transformations. The known iron sulfide minerals, their structures and stabilities are summarized in Table 1. Detailed accounts of the mineral chemistry of these sulfides are provided by WARD (1970), POWER and FINE (1976), VAUGHAN and CRAIG (1978), VAUGHAN and LENNIE (1991).

Formation of iron-sulfur phases is affected by the d-electron configuration of Fe, resulting in a more complex range of structures than would be otherwise expected. As an example of this, the formation of (metastable) marcasite (FeS_2) from acidic aqueous solution has been explained by the effect of bonding of H^+ at the crystal surface on the Fe 3d electronic structure. We were interested in examining the formation of the reduced phase(s) to determine if electron withdrawing effects might also be responsible for formation of Cubic FeS and troilite, both of which, like marcasite, show pH-dependant formation.

In the present article, we examine the monosulfide mackinawite and explore the properties of "amorphous FeS" as a key to understanding the

formation of mackinawite, Cubic FeS and troilite. This work forms part of a series of contributions to studies of the crystal chemistry and phase relations of the iron sulfides (LENNIE, 1994; LENNIE *et al.* 1995a, 1995b).

MACKINAWITE

Mackinawite possesses a layer structure similar to that found in tetragonal lead oxide (see Table 1) with Fe and S occupying the sites of O and Pb, respectively, in PbO . Here we investigate further the oxidation state and local structure of Fe and S in synthetic mackinawite.

Synthesis

Several different methods for synthesis of mackinawite have been described in the literature. BERNER (1964) found that reaction of metallic Fe with a saturated solution of H_2S gave well crystallised tetragonal FeS. Alternatively, mackinawite has been prepared by reacting aqueous solutions of Fe(II) ions and HS^- ions forming an X-ray amorphous precipitate which, even on ageing, gives a poorly crystalline mackinawite.

In the present work, sulfidation of a commercial iron wire (Roncraft, Sheffield) was used to produce crystalline mackinawite. Here, a solution of Na_2S was added slowly to an 0.5 molar acetic acid/acetate buffer ($\text{pH} = 4.6$) in which approximately 4–5g of finely divided iron wire had been previously immersed. Dissolution of the iron wire by reaction with the acetate buffer for 30 minutes or so evolved H_2 , providing a reducing solution environment. The Na_2S solution was then added slowly, and exceeded the capacity of the acetate buffer, increasing the pH to a value of approximately $\text{pH} = 6.5$. This solution, containing the iron wire, was allowed to stand for 24 hours. The generated H_2 trapped in the wool mat floated the iron to the top of the solution. Mackinawite forming on the iron surface spalled off and dropped to the bottom of the flask. After reaction, the remaining iron wool was removed, the supernatant solution poured off, and the mackinawite carefully rinsed then dried under vacuum. Samples were sealed under vacuum in glass tubes until required for further analysis.

Crystal structure

The mackinawite synthesised as described above was examined using high resolution X-ray powder diffraction from which a Rietveld structure refinement was obtained. The structural parameters

Table 1. The iron sulfides, their structures, stabilities and natural occurrence*

Composition mineral	Crystal structure type structural data †	Stability ‡	Natural occurrence
FeS ₂ pyrite	pyrite-type (cubic) <i>Pa3</i> ; <i>a</i> = 5.42	stable (<742°C)	The most abundant sulfide. Found as an accessory mineral in many igneous, metamorphic and sedimentary rocks including coals. The major sulfide in many massive, bedded or vein type ores.
FeS ₂ marcasite	marcasite-type (orthorhombic) <i>Pnm</i> ; <i>a</i> = 4.44; <i>b</i> = 5.41; <i>c</i> = 3.38	metastable	Occurs as a primary mineral in certain sediments and lower temperature hydrothermal deposits. Also formed through weathering of other sulfide minerals.
Fe ₃ S ₄ greigite	spinel-type (cubic) <i>Fd3m</i> ; <i>a</i> = 9.88	metastable	A very rare mineral reported from Recent sediments and low temperature hydrothermal deposits.
~Fe ₉ S ₁₁ (?) smythite	?pseudorhombohedral <i>a</i> = 3.47; <i>c</i> = 34.4	?stable (~ 75°C)	A very rare (?) mineral reported from magmatic and hydrothermal sulfide ore deposits.
~Fe ₇ S ₈ monoclinic pyrrhotite	NiAs-type; superstructure (mono.) <i>F2/d</i> ; <i>a</i> = 11.90; <i>b</i> = 6.86; <i>c</i> = 22.79; β = 90°26'	?stable ~254°C	As an important mineral in sulfide ores of 'magmatic' origin and an accessory mineral in ultramafic and mafic rocks. Also in metamorphosed massive sulfides and some hydrothermal ores.
Fe ₉ S ₁₀ intermediate pyrrhotite (5C)	NiAs-type; superstructure (hexagonal) <i>a</i> = 6.88; <i>c</i> = 28.70	?stable (? ~ 100°C)	"
Fe ₁₀ S ₁₁ intermediate pyrrhotite (11C)	NiAs-type; superstructure (orthorhombic) <i>Cmca</i> or <i>C2Ca</i> ; <i>a</i> = 6.89; <i>b</i> = 11.95; <i>c</i> = 63.18	?stable (? ~ 100°C)	"
Fe ₁₁ S ₁₂ intermediate pyrrhotite (6C)	NiAs-type; superstructure (hexagonal) <i>a</i> = 6.89; <i>c</i> = 34.48	?stable (? ~ 100°C)	"
~Fe ₉ S ₁₀ -Fe ₁₁ S ₁₂ non-integral pyrrhotite (nC)	NiAs-type; superstructure (orthorhombic or monoclinic); <i>a</i> = 6.89; <i>b</i> = 11.95; <i>c</i> = variable	?stable (? ~ 220°C)	"
FeS troilite	NiAs-type (distorted super- structure) (hexagonal) <i>P62c</i> ; <i>a</i> = 5.97; <i>c</i> = 11.75	stable (<138°C)	Found in iron meteorites and lunar rocks. Rare on Earth but found in some serpentinized ultramafic rocks.
Fe _{1+x} S (<i>x</i> = 0.01-0.08) mackinawite	PbO-type (tetragonal) <i>P41nm</i> ; <i>a</i> = 3.60; <i>c</i> = 5.03	metastable	As the first-formed very fine grained black sulfide precipitated in Recent sediments. Also as small grains and lamellae within other sulfides (pyrrhotite, chalcopyrite etc.) from a variety of environments.
Fe _{1+x} S (<i>x</i> = 0.03-0.10) cubic FeS (synthetic)	Sphalerite-type (cubic) <i>F43m</i> ; <i>a</i> = 5.42	metastable	Known only from synthetic studies at present and formed as a layer on sulfidized iron surfaces.

* Data from Vaughan and Craig (1978), Kissin and Scott (1982)

† Information given is on structure type (crystal class); space group; unit cell parameters (in Å)

‡ Upper temperature of stability in parentheses

obtained from this refinement, reported elsewhere (LENNIE *et al.*, 1995b), are given in Table 2.

X-ray photoelectron spectra

X-ray photoelectron spectra were obtained on a Kratos XSAM 800 surface analysis system op-

erating at a base pressure of less than 1×10^{-9} τ . Removing mackinawite from the glass tube and subsequent transfer into the spectrometer vacuum chamber was carried out under O₂-free N₂ conditions. Narrow region XPS spectra were recorded at an analyser pass energy of 20 eV. The spectrometer was calibrated using the peaks: Au (4f_{7/2}) 84.00

Table 2. Refined structure parameters for synthetic mackinawite. Errors (σ) are in parentheses (after LENNIE *et al.*, 1995b)

Space group	<i>PA/nmm</i> (No. 129) origin at $\bar{4}m2$			
Cell parameters (Rietveld)	<i>a</i> (Å)	3.6735(4)		
	<i>b</i> (Å)	3.6735(4)		
	<i>c</i> (Å)	5.0328(7)		
	<i>V</i> (Å ³)	67.914(24)		
Atomic positional parameters	<i>x</i>	<i>y</i>	<i>z</i>	<i>B</i> (iso)
Fe in 2(a):	0	0	0	0.41(2)
S in 2(c):	0	0.5	0.2602(3)	0.20(2)
Bond distances (Å)				
Fe-S:	2.2558(9)			
Fe-Fe:	2.5976(3)			

eV, Cu ($2p_{3/2}$) 932.66 eV, Ag ($3d_{5/2}$) 368.27 eV with Mg $K\alpha$ X-rays (1253.6 eV) as the exciting radiation, and the static charge effect was corrected using adventitious C with the 1s electron binding energy of C taken as 284.6 eV. For comparison with mackinawite, XPS measurements were also made on a natural sample of pyrite cleaved under O₂-free N₂ conditions prior to installation in the spectrometer. A succession of spectra of the cleaved pyrite were taken before, and after, a series of Ar⁺ etches of the surface. Fig. 2 shows the Fe, S and O XPS spectra obtained for synthetic mackinawite. These spectra are fitted using a Shirley background (SHIRLEY, 1972).

The Fe ($2p_{3/2}$) peak of mackinawite has a binding energy of 707.25 eV, similar to that of pyrite (707.2 eV), which provides confirmation of the Fe(II) oxidation state predicted for mackinawite. The mackinawite Fe($2p_{3/2}$) peak shows considerable asymmetric broadening at the higher binding energy side of this peak, which may arise from the high conductivity (WERTHEIM and BUCHANAN, 1977) in the (001) plane of mackinawite due to Fe-Fe interactions inferred by KJEKSHUS *et al.* (1972).

Following background subtraction, the S (2p) photoelectron spectrum of mackinawite has been fitted with a doublet in a 2:1 ratio to match the 2:1 intensity ratio of the spin-orbit splitting of S ($2p_{3/2}$) and $2(p_{1/2})$ peaks. These have been fitted with asymmetric curves made up of symmetric 80% Gaussian, 20% Lorentzian components. The binding energies of the fitted doublet are 161.82 eV and 163.02 eV for the $2(p_{3/2})$ and $2(p_{1/2})$ peaks respectively. The O (1s) spectrum in Fig. 2 shows the small fraction of O in the sample of mackinawite. The peak position (532 eV) is consistent

with the presence of iron hydroxide on the surface of mackinawite (MCINTYRE and ZETARUK, 1977).

The pyrite XPS Fe ($2p_{3/2}$) spectrum binding energy is 707.2 eV, and the S(2p) spectra were fitted with symmetric Gaussian 50%, Lorentzian 50% curves at 162.5 eV and 163.7 eV respectively. Following Ar⁺ etching, the Fe ($2p_{3/2}$) peak showed considerable broadening and increased asymmetry towards the higher binding energy side of this peak. The S(2p) spectrum showed formation of additional peaks at lower binding energies which were fitted with symmetric Gaussian 50%, Lorentzian 50% curves at 161.3 eV and 162.5 eV respectively. These changes in Fe and S photoelectron peaks are consistent with the partial reduction of S₂²⁻ to S²⁻ species, and partial oxidation of Fe(II) which would occur upon reduction to pyrrhotite. The S($2p_{3/2}$) peak of pyrite (S²⁻) has a higher binding energy (162.5 eV) than that observed for S (S²⁻) in mackinawite (161.85 eV), consistent with observed trends which show increasing binding energy with increase in formal oxidation state.

The binding energy may also reflect differences in the lattice site environment between two different phases of the same oxidation state. In the case of mackinawite, S (S²⁻) is coordinated to four Fe atoms in a pyramidal arrangement, with a lone pair of electrons at the apex of this pyramid. In contrast, S in pyrrhotite (S²⁻) is coordinated to 6 Fe atoms in a trigonal prism arrangement. The binding energy of S in mackinawite (161.85 eV) is greater than the binding energies reported for pyrrhotite phases (161.1 - 161.25). This suggests a slight decrease in the electronic population of the S valence band(s) for mackinawite compared with that of the S valence band(s) for the pyrrhotites.

A compilation of S ($2p_{3/2}$) and Fe ($2p_{3/2}$) binding energies reported in the literature for Fe-S minerals, together with those obtained for pyrite and mackinawite from our experiments, is presented in Table 3.

X-ray absorption spectra

X-ray absorption spectroscopy (XAS) and the analysis of the fine structure in spectra at and near the absorption edge (so called 'XANES'), and in the energy region extending well above the edge (so-called 'EXAFS'), have been very comprehensively described in the literature (see CALAS *et al.* 1984, 1990; BROWN *et al.*, 1988; WAYCHUNAS and BROWN, 1984, for excellent reviews). Here only specific details of our experiments and their interpretation will be discussed.

Mackinawite was examined by X-ray Absorp-

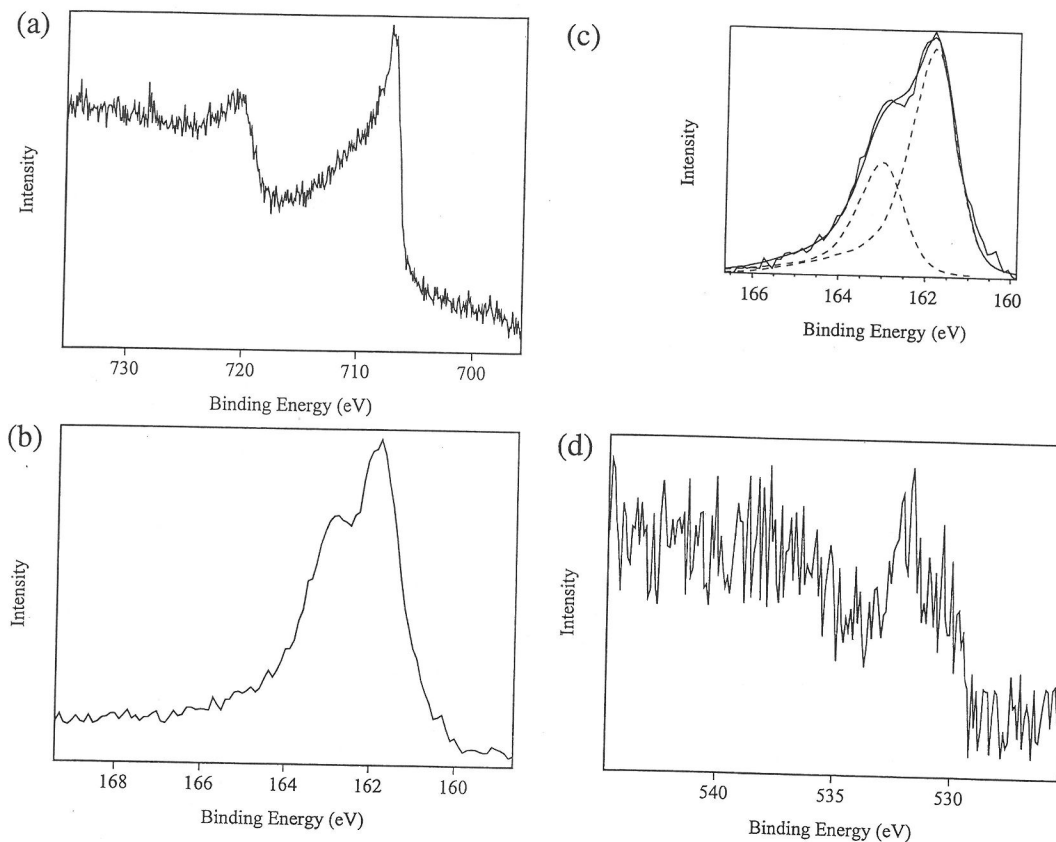


FIG. 2. XPS spectra of synthetic mackinawite: (a) Fe (2p) spectrum and (b) S (2p) spectrum. (c) The S (2p) spectrum following background subtraction and fitted with a doublet of asymmetric curves at 161.82 eV ($2p_{3/2}$) and 163.02 eV ($2p_{1/2}$). (d) O (1s) spectrum: the small fraction of oxygen in the synthetic material, due to surface hydroxide species, is indicated by the low signal to noise ratio.

Table 3. XPS binding energies of S ($2p_{3/2}$) and Fe ($2p_{3/2}$) found in iron-sulfur minerals, including results from this study

Species	Mineral	Binding energy (eV)	Reference
Fe ($2p_{3/2}$)	FeS ₂ (pyrite)	707	BUCKLEY and WOODS (1987)
		707.2	this study
	Fe _{1+x} S (mackinawite)	707.25	this study
	Fe _{0.89} S (pyrrhotite)	708	BUCKLEY and WOODS (1985)
	Fe ₇ S ₈ (pyrrhotite)	707.45	PRATT <i>et al.</i> (1994)
	Ar ⁺ reduced FeS ₂ surface	707.8	this study
S($2p_{3/2}$)	S(0)	163.7	HYLAND and BANCROFT (1989)
	FeS ₂ (pyrite)	162.3	BUCKLEY and WOODS (1987)
		162.4	HYLAND and BANCROFT (1989)
		162.5	this study
	Fe _{1+x} S (mackinawite)	161.82	this study
	Fe _{0.89} S (pyrrhotite)	161.1	BUCKLEY and WOODS (1985)
	Fe ₇ S ₈ (pyrrhotite)	161.25	PRATT <i>et al.</i> (1994)
	Ar ⁺ reduced FeS ₂ surface	161.24	this study

tion Spectroscopy using synchrotron radiation to establish the local environment around Fe and S, and to provide model XAS data for amorphous iron sulfide precipitates. To obtain Fe K-edge absorption data, a solid synthetic mackinawite sample was pressed into Al samples holders with adhesive-tape windows and cooled under vacuum using a liquid N₂ cryostat. The spectrum for Fe was collected in transmission mode on Station 7.1 at the Daresbury Synchrotron Radiation source, operating at 2 GeV with an average current of 150 mA. A Si(111) double-crystal monochromator was used with the crystal faces offset to give 50% rejection of the beam in order to reduce harmonic contamination. Ion chambers to detect the incident and transmitted radiation were filled with Ar-He mixtures to absorb 20% and 80% of the beam, respectively.

The spectrum for S was taken on Station 3.4 using a Ge(111) double crystal monochromator; a focussing mirror is used to remove higher harmonics. The sample of synthetic mackinawite was diluted with graphite and coated as a slurry in acetone onto aluminium stubs. Following evaporation of the acetone, the stubs were mounted in the spectrometer and the chamber evacuated. Spectra over the S K-edge were taken using photo-electron yield as the detection technique. In the case of the S spectrum, four separate scans were summed to improve the signal to noise ratio.

Spectra were prepared for analysis by background subtraction of pre-edge and EXAFS regions of the spectra, followed by normalisation using the Daresbury programs, EXCALIB and EXBACK (DAIKUN *et al.*, 1984). Standard k^3 weighting was used for the EXAFS spectra. The data were analysed using single-scattering curved wave theory in the program EXCURV92 (BINSTED *et al.*, 1991; LEE and PENDRY, 1975; GURMAN *et al.*, 1984, 1986). Phase shifts are derived from *ab initio* calculations within EXCURV92 using the default parameters for the muffin tin radii and exchange terms. The phase shifts were not further refined using model compounds.

A fit was produced by generating a theoretical spectrum from a structure of several shells of back-scatterers around the central atom, and allowing parameters refining radial distance from the central scattering atom and Debye-Waller factors within each shell to vary iteratively to give the best agreement with the experimental data. Coordination numbers were kept fixed for analysis of synthetic mackinawite, and only those shells that made a significant improvement to the fit were included in the simulations. The goodness of fit of the theoretical spectrum to the experimental data is given

by $R(\min)$, the value of the fit index at predicted minimum (JOYNER *et al.*, 1987).

Fig. 3 shows k^3 weighted spectra from EXCURV92 for S and Fe of mackinawite plotted against the inverse wave-vector, k , and Fourier transforms of these spectra giving the radial distance from the central scattering atoms. Data obtained from the iterative fitting of these spectra are given in Table 4. Both S K-edge and Fe K-edge spectra have been fitted with three shells. The model set up for the S K-edge data uses an approximation for the second and third shells—the second shell was modelled by 12 S atoms at 3.62 Å (instead of 4 S at 3.548 Å, 4 S at 3.674 Å and 4 S at 3.688 Å); the third shell by 12 Fe atoms at 4.26 Å (not 4 Fe at 4.153 and 8 Fe at 4.311). Distances and coordination numbers for initial fitting were calculated from the structural refinement of mackinawite presented in Table 2.

The results of these iterative fits to the Fe K-edge and S K-edge EXAFS spectra of mackinawite are consistent with the structure determined by X-ray powder diffraction, and confirm both the tetrahedral coordination of Fe by S, and the short Fe-Fe distances in the (001) plane of mackinawite.

AMORPHOUS IRON SULFIDE ("FeS")

The material initially formed when dissolved Fe and S react in solution is an extremely fine-grained "X-ray amorphous" black precipitate. Such amorphous iron sulfide precipitates, which are easily prepared in the laboratory, form in nature by reactions taking place in Recent sediments, principally during processes that take place just beneath the surface of certain fine sediments during early diagenesis. Here, the most common interactions involve sulfide S derived from reduction of seawater sulfate by bacteria, and Fe from detrital or other sources.

These fine grained materials are difficult to study using techniques such as X-ray diffraction or electron microprobe analysis. In our work, we have used X-ray Absorption Spectroscopy employing synchrotron radiation to study the structure of these precipitates. This work has involved attempts to study such precipitates by quenching in liquid N₂ immediately following nucleation, after controlled periods of "ageing", and following buffering in a range of solution pH's.

FeS Amorphous Precipitates; Ageing Experiments

A series of FeS precipitates were prepared as follows. Equal volumes of an Fe acetate solution

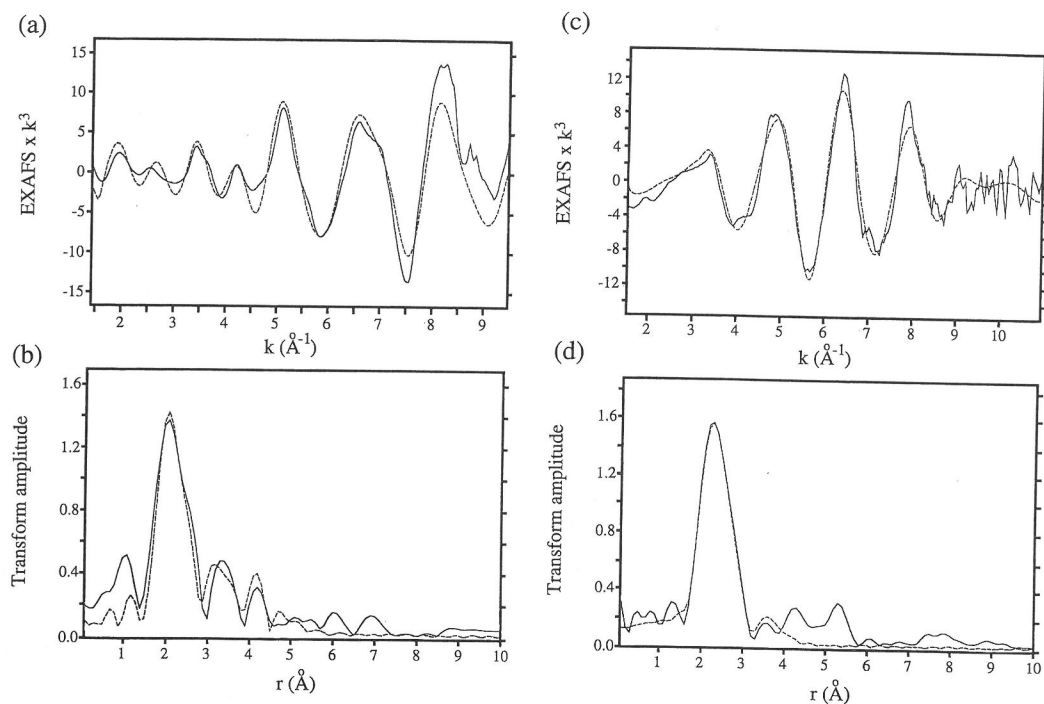


FIG. 3. (a) The k^3 -weighted S K-edge EXAFS spectrum of mackinawite (298 K). (b) The Fourier transform of the S K-edge EXAFS spectrum fitted with three shells (as listed in Table 4). (c) The k^3 -weighted Fe K-edge EXAFS spectrum of mackinawite (liq. N_2 cooled). (d) The Fourier transform of the Fe K-edge EXAFS spectrum fitted with three shells (as listed in Table 4). Solid lines, experimental data; dashes, data simulated in EXCURV92.

Table 4. Results of refinements of EXAFS S K-edge and Fe K-edge spectra for mackinawite

Central Atom	Shell	Element	$r(\text{\AA})$	$A: 2\sigma^2(\text{\AA}^2)$	N	$r_{\text{XRD}}(\text{\AA})$	N_{XRD}
S (298 K) [R(min) = 14.9]	1	Fe	2.24	0.01	4	2.255	4(Fe)
		S	3.62	0.03	12	3.548	4(S)
							3.674
	3	Fe	4.26	0.04	12	3.688	4(S)
						4.153	4(Fe)
						4.311	8(Fe)
Fe (298 K) [R(min) = 7.7]	1	S	2.26	0.03	4	2.255	4(S)
	2	Fe	2.56	0.03	4	2.598	4(Fe)
	3	Fe	2.59	0.02	4	2.255	4(S)
3.68			0.03	4	2.598	4(Fe)	
					3.674	4(Fe)	

r = radial distance of fitted shell from central atom; A = Debye-Waller factor

N = coordination number; $R(\text{min})$ is the value of the fit index at predicted minimum

r_{XRD} = radial distance from central atom calculated from XRD data in Table 2

N_{XRD} = coordination number of element (in brackets) calculated from XRD data in Table 2

(0.05 molar) and a 1:1 mixture of 1N NaOH and a solution 0.21 molar in $\text{Na}_2\text{S}\cdot 9\text{H}_2\text{O}$ were injected at the same time directly into polyethylene tubes sealed at one end. The solution pH above the precipitates thus formed was 7.5. After measured time periods (1, 5, 10, 20, 60, 300 and 1800 seconds), the tubes containing the precipitates were plunged into liquid nitrogen to quench the reaction. Rapid quenching also limits the formation of ice-crystals which would give Bragg reflections in the absorption experiments. Acetate was selected as the anion in these experiments to prevent confusion with sulfide during EXAFS analysis. Cl^- as an anion was avoided as this has similar X-ray scattering properties to S, being close in atomic mass.

At Daresbury, the tube containing the frozen precipitate was cut to provide a 2.5 cm length of tubing plus precipitate. The frozen precipitate contained within this length was removed and installed in an aluminium holder which was placed in a liquid N_2 cryostat and evacuated to 10^{-4} mbar. Fe K-edge XAS measurements were made in fluorescence mode on Station 8.1 by detecting fluorescence using the Canberra solid state detector.

These spectra, the XANES region for which are shown in Fig. 4, have been analysed using EXCURV92 as described above. The coordination number has also been allowed to vary during iteration. Data obtained from these fits are given in Table 5. These show that a precipitate is rapidly formed which has Fe tetrahedrally coordinated by a first shell of S, and a second shell of Fe atoms with short distances (2.59\AA) from the central Fe atom. These radial distances are consistent with formation of a mackinawite-type structured phase as early as 1 second after initial reaction. The qual-

ity of data obtained for 10 and 20 seconds ageing time is not sufficient to provide second shell information for these samples.

FeS Amorphous Precipitates; pH Buffering Experiments

A series of 'FeS' solids were precipitated, then buffered as follows at different pH values. Iron acetate solution (1.6 mls, 0.05 M) was added to 3 mls of a solution 0.21 molar in $\text{Na}_2\text{S}\cdot 9\text{H}_2\text{O}$. This mixture gave a black amorphous FeS precipitate; the resulting solution pH was 4.5. Buffering to higher pH values, as determined by pH meter, was achieved by adding drops of a 1N NaOH solution. The lower pH (3.9) was achieved by addition of acetic acid.

The precipitate, with buffering solution, was injected into a polyethylene tube sealed at one end, held for 15 mins. at 298 K, then plunged into liquid N_2 to quench the reaction. Spectra over the Fe K-edge were then taken on Station 8.1 as described in the previous section. No S K-edge EXAFS spectra have been taken of the pH buffered or quenched amorphous precipitate experiments as the Station 3.4 spectrometer design prevents analysis of frozen precipitates.

Data obtained from analysis of these Fe K-edge spectra using EXCURV92 are given in Table 6. Again, the coordination number has been allowed to vary during iteration. The XANES region of these spectra are shown in Fig. 5. These precipitates show ordering after 15 minutes reaction sufficient to provide second shell information, and indicate formation of a mackinawite-like structure for precipitates buffered at pH's of 4.5 and above. The results for the precipitate buffered to pH 3.9, which has been fitted with two S shells surrounding the Fe atom, may have been affected by partial oxidation of sulfide during addition of acetic acid to achieve the required pH.

The data obtained from these pH buffered precipitates do not show obvious changes in coordination of Fe by S between pH 4.5 and 6.5; there is no evidence of 6-fold coordination of Fe by sulfur in these amorphous precipitates. We will refer to this result in the following discussion of a possible mechanism of formation for the phases Cubic FeS and troilite in the region of pH 4–5.

METASTABLE Fe-S PHASE RELATIONS

Formation of Cubic FeS and troilite from aqueous solution

Cubic FeS, a metastable synthetic iron sulfide with the sphalerite structure, first reported by

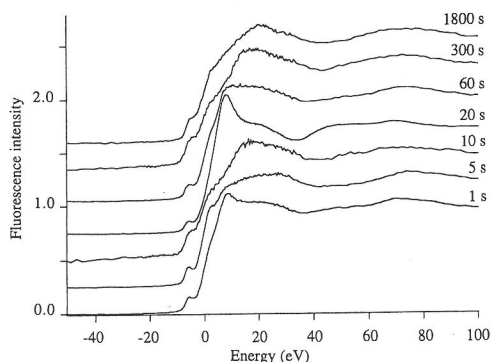


FIG. 4. Edge region Fe K-edge fluorescence spectra of iron sulfide precipitate ageing experiments. The energy scale (eV) is set so that the Fe K adsorption edge is at 0 eV.

Table 5. Results of refinements of Fe K-edge EXAFS spectra for quenched reaction time iron sulfide precipitates

FeS precipitate	Shell	Element	r (Å)	A: $2\sigma^2$ (Å ²)	N
1 second [R(min) = 44.3]	1	S	2.24	0.02	3.8
	2	Fe	2.59	0.02	2.0
5 seconds [R(min) = 38.1]	1	S	2.22	0.02	3.8
	2	Fe	2.57	0.02	2.8
10 seconds [R(min) = 63.5]	1	S	2.26	0.01	3.0
20 seconds [R(min) = 46.5]	1	S	2.25	0.01	3.4
60 seconds [R(min) = 52.7]	1	S	2.20	0.02	3.9
	2	Fe	2.59	0.03	3.5
300 seconds [R(min) = 54.3]	1	S	2.23	0.01	4.0
	2	Fe	2.68	0.02	2.5
1800 seconds [R(min) = 39.7]	1	S	2.21	0.02	4.0
	2	Fe	2.62	0.02	2.8

r = radial distance of fitted shell from central Fe atom; A = Debye-Waller factor
N = coordination number; R(min) is the value of the fit index at predicted minimum

DE MEDICIS (1970 a, b), was synthesised by reacting Fe metal at 298 K with aqueous H₂S solutions having pH values between 4.0 and 4.5. TAKENO *et al.* (1970) synthesised Cubic FeS by reacting Fe metal with H₂S in solution at 323 K and report X-ray powder diffraction data for Cubic FeS synthesised in solutions with a pH of 5.7. These authors observed that euhedral troilite (and anhedral mackinawite) are also formed under the acidic reducing conditions required for Cubic FeS formation.

SHOESMITH *et al.* (1980) showed that formation of both troilite and Cubic FeS from stainless steels corroded by aqueous sulfide solutions at 294 K shows similar dependence on solution pH. Cubic FeS formed in greater quantities than troilite with the quantity of troilite and Cubic FeS formed being greatest at pH's between 4 and 5. At higher pH, mackinawite is the predominant iron sulfide formed while at lower pH, all these iron monosulfide phases readily dissolve. MUROWCHICK and BARNES (1986a) found similar pH dependant distri-

Table 6. Results of refinements of Fe K-edge EXAFS spectra for pH buffered iron sulfide amorphous precipitates

FeS precipitate	Shell	Element	r (Å)	A: $2\sigma^2$ (Å ²)	N
pH 3.9 [R(min) = 42.6]	1	S	2.20	0.01	4
	2	S	2.37	0.01	2
pH 4.5 [R(min) = 46.1]	1	S	2.25	0.01	4
	2	Fe	2.67	0.02	3
	3	S	4.24	0.02	8
pH 5.4 [R(min) = 48.7]	1	S	2.19	0.01	4
	2	Fe	2.61	0.02	4
pH 6.5 [R(min) = 40.3]	1	S	2.25	0.01	4
	2	Fe	2.68	0.03	4
pH 7.4 [R(min) = 38.5]	1	S	2.23	0.01	4
	2	Fe	2.65	0.03	2.7

r = radial distance of fitted shell from central Fe atom; A = Debye-Waller factor
N = coordination number; R(min) is the value of the fit index at predicted minimum

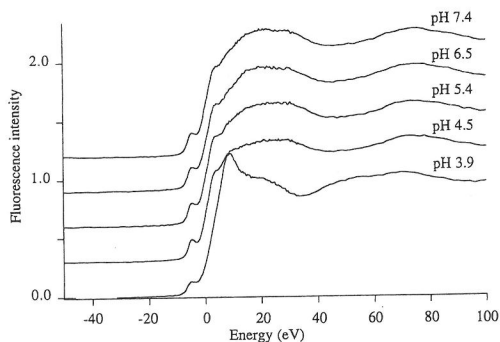


FIG. 5. Edge region Fe K-edge fluorescence spectra of pH buffered iron sulfide precipitates. The energy scale (eV) is set so that the Fe K adsorption edge is at 0 eV.

butions of troilite and Cubic FeS formation when Fe metal was sulfidised by aqueous H_2S in experiments carried out in solutions covering a pH range from 2 to 7, and between 328 K to 366 K.

Although troilite and above 413 K, stoichiometric hexagonal pyrrhotite, are considered stable phases in the Fe-S system, formation of the less S-rich pyrrhotites from aqueous solution under equilibrium conditions (hydrothermal synthesis) is prevented due to the unmanageably high H_2 pressures generated by dissociation of H_2O at low S fugacity (KISSIN and SCOTT, 1982). Troilite is therefore formed under non-equilibrium conditions in the above experimental studies.

Cubic FeS spontaneously transforms to mackinawite at room temperature. SHOESMITH *et al.* (1980) measured the rate of this solid state transformation at 298 K using changing intensities of X-ray diffraction peaks, and proposed a mechanism involving migration of Fe atoms for this transformation. Although no measurements have been made of the temperature dependence of the rate of this transformation, the observation that Cubic FeS does not persist above 366 K (MUROWCHICK and BARNES, 1986a) implies extremely rapid transformation at or above this temperature. There are small deviations from a stoichiometric formula of FeS reported in the literature for both Cubic FeS and mackinawite, which may indicate either iron excess or sulfur deficiency in these phases. However, the crystallographic origin of these compositional variations has not been definitely established.

Proposed mechanism of formation of Cubic FeS and troilite from solution

We now propose a mechanism to explain the similar dependence on pH of both Cubic FeS and

troilite formation. We first refer to a study by TOSSELL *et al.* (1981) which accounted for pH dependant formation of marcasite by suggesting that interaction of surface bound H^+ with electrons in one of the $1\pi_g^*$ molecular orbitals of S_2^{2-} would effectively remove 2 electrons from the $M3d\sigma-A_21\pi_g^*$ system, distorting the S geometry around each Fe. Metastable marcasite would thus be formed in preference to stable pyrite.

We propose that a similar electronic effect may also be occurring in the formation of Cubic FeS and troilite under acidic conditions. At pH's between 4–5, H^+ ions bound to S at the surface of the iron monosulfide would act to withdraw electrons from Fe 3d orbitals. Ferrous ions ($3d^6$) would assume $3d^5$ character, thus making this Fe isoelectronic with Mn^{2+} . It has been observed that in the Mn-S system, two metastable phases, β -MnS and γ -MnS, form by precipitation with H_2S gas from aqueous manganous solutions (FURUSETH and KJEKSHUS, 1965). These phases have sphalerite and wurtzite structures respectively: there are no NiAs-type or tetragonal PbO-type structures found in the MnS system.

If Fe ions at the surface of a FeS crystal growing in acidic solution are assumed to have $3d^5$ character as proposed above, formation of FeS under these conditions may be expected to result in iron monosulfides having sphalerite and wurtzite structures, as found for β -MnS and γ -MnS. Cubic FeS formed under acidic conditions has the sphalerite structure, in agreement with this theory. However, there are no reports in the literature of wurtzite-type FeS formed under acidic conditions. Instead, it is troilite (with a distorted NiAs-type structure) which is observed under these conditions.

We note however that both NiAs and wurtzite-type structures have a hexagonal close-packed anion sublattice, as shown in Fig. 6. The arrangement of Fe (in hexagonal pyrrhotite/troilite) and Zn (in wurtzite) are different; Fe occupies octahedral sites in troilite, whereas in wurtzite, Zn atoms are in tetrahedral sites.

By analogy with Cubic FeS, which transforms spontaneously to mackinawite by rearrangement of Fe, a rapid solid-state transformation at the crystal surface from a (hypothetical) wurtzite-type FeS structure to FeS-troilite, after the removal of electron withdrawing H^+ ions from the surface, would explain both the absence of a wurtzite-type FeS and the presence of troilite in the experiments referred to above. The degree of rearrangement of Fe required for transformation of a wurtzite-type FeS to troilite would be much smaller than that

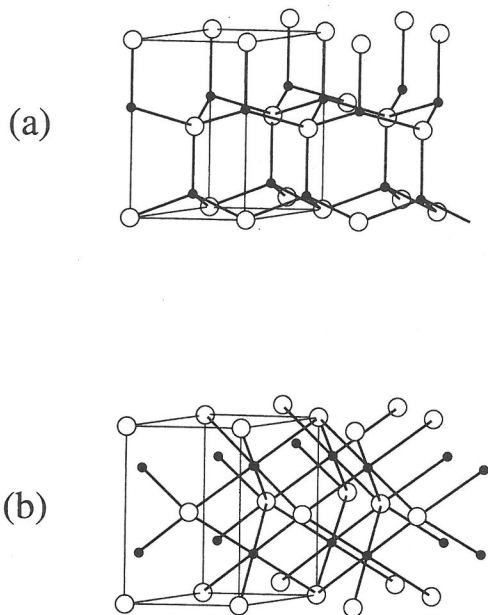


FIG. 6. Crystal structure diagrams for (a) wurtzite, the proposed structure for the metastable hexagonal FeS precursor, and (b) the NiAs structure which forms the basis of troilite and hexagonal pyrrhotite. In (a), open circles represent S while filled circles represent Zn (Fe). In (b), open circles represent As (S), while filled circles represent Ni (Fe).

for transformation of Cubic FeS to mackinawite (see Fig. 6). This proposed transformation would therefore be much more rapid than the observed, spontaneous, transformation of Cubic FeS to mackinawite.

Spontaneous transformation of Cubic FeS to mackinawite (and of a wurtzite-type FeS to troilite) indicates that electrons surplus to eight valence electrons per formula unit are accommodated by structural rearrangements which increase electronic stability. In sphalerite (ZnS), structural stability is achieved because all low-energy molecular orbitals are occupied and a large energy gap is present between highest occupied and lowest unoccupied molecular orbitals (TOSSELL and VAUGHAN, 1992). Electronic structure models for the FeS phases Cubic FeS and mackinawite (WELZ and ROSENBERG, 1987) show that mackinawite has a reduced density of states at the Fermi level when compared with Cubic FeS. This increased band width of mackinawite is due to contributions from both Fe *d* and S *p* orbitals. Considerable Fe-Fe interaction between edge sharing FeS₄ tetrahedra in mackinawite causes a rearrangement and splitting of the Fe *d*-orbitals while the increased band width of S *p* orbitals is

ascribed to strong deviation of the S environment from cubic to pyramidal symmetry, and to direct S-S contact between Fe-carrying sheets. These changes in electronic and crystal structure thus give mackinawite greater stability than Cubic FeS. For the purposes of electronic structure modeling, WELZ and ROSENBERG (1987) assumed stoichiometric compositions for both Cubic FeS and mackinawite.

BURDETT (1980) uses fragment formalism to view the structure of some simple ('AX') solids in terms of the packing of planar hexagonal sheets and their puckered analogues. The wurtzite structure, often regarded as a metastable version of the sphalerite arrangement, is, in general, found for four-coordinate structures with the largest electronegativity difference (Δ_x) between A and X. Burdett finds that the energy difference between these two AX structures decreases as the electronegativity of X increases. As Δ_x increases further, the rocksalt structure is produced, as shown by Pearson diagrams (PEARSON, 1962).

Solids having more than 8 valence electrons per AX unit adopt structures that may be understood via bond-breaking processes of the electron-precise wurtzite structure (BURDETT, 1980). Thus, Burdett argues that the NiAs-type structure can be generated by considering the effect of adding electrons to an 'AX' puckered sheet structure. Following these arguments presented by Burdett, we propose that introduction of additional electrons into the 8 electron structural framework of (hypothetical) 'wurtzite-type FeS' is the driving force for transformation to a NiAs-type FeS.

Thus our model for iron monosulfide formation can be used to explain the origin of all three different FeS crystal structures (troilite, Cubic FeS, mackinawite) from Fe tetrahedrally coordinated by S. This proposed mechanism overcomes several difficulties. Previous studies have shown that the initial amorphous FeS precipitate formed on reaction of aqueous Fe(II) and dissolved sulfide ages to form mackinawite (BERNER, 1964; RICKARD, 1989), and from EXAFS evidence (PARISE and SCHOONEN, 1991; this study), we know that tetrahedral nucleation of Fe by S in reducing solutions develops rapidly. Hence, we consider it unlikely that direct troilite nucleation from solution species with Fe coordinated by 6 S atoms occurs. By showing that troilite could nucleate from solution via Fe tetrahedrally coordinated by S, we avoid the need for solution complexes, such as the trimeric Fe₃S₃ precursor proposed by TAYLOR (1980), as species required for troilite formation.

Our model may also be used to interpret the

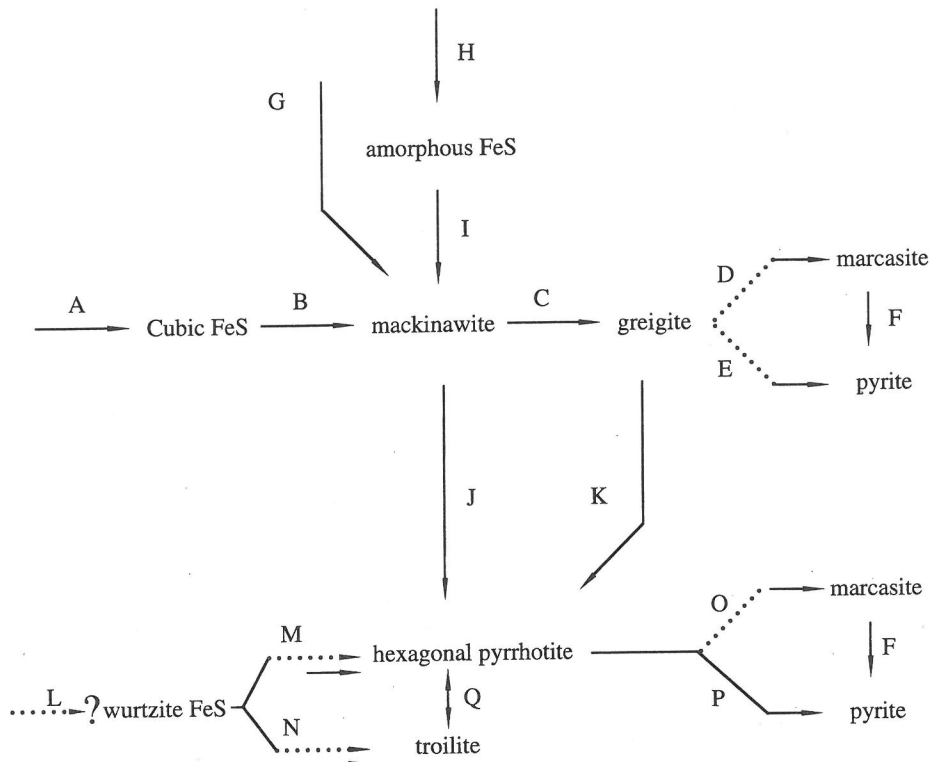


FIG. 7. Summary of known, and speculative phase transformations and formation reactions in the low temperature iron-sulfur system. Transformations that have not been directly demonstrated experimentally are shown by dotted lines. The key to the letters in this figure is given below: A. Formation from Fe^{2+} or Fe, and HS^- or H_2S , pH 4–5 (<368 K); MUROWCHICK and BARNES (1986a). B. Solid state transformation, kinetics only partially established, see SHOESMITH *et al.* (1980). C. Solid state transformation involving oxidation (of Fe), no kinetic data available; see TAYLOR *et al.* (1979b). D. Inferred reaction, by sulfidation of greigite, at pH <5 , $T<523$ K; MUROWCHICK and BARNES (1986b). E. Inferred reaction, by sulfidation of greigite, at pH >5 , $T<523$ K; MUROWCHICK and BARNES (1986b). For kinetics of pyrite formation from iron monosulfide precursors, see RICKARD (1975). F. Solid state transformation, for kinetics of this reactions, see LENNIE and VAUGHAN (1992), structural aspects described by FLEET (1970). G. Sulfidation of Fe, by HS^- or H_2S , pH in range 3–10 ($T<523$ K). H. Precipitation from Fe^{2+} , by HS^- or H_2S , pH in range 3–10 ($T<523$ K). I. Ageing of amorphous precipitate, see BERNER (1964). J. Solid state transformation; kinetics described in LENNIE *et al.* (1995a). K. Solid state transformation, kinetics not established. L. Precipitation from Fe^{2+} , by HS^- or H_2S , pH in range 4–6 wide range of temperatures, to above 573 K. Wurtzite-type FeS phase speculated, see this study. M & N. Formation of either hexagonal pyrrhotite (>413 K) M, or troilite (<413 K) N from Fe^{2+} and HS^- or H_2S between pH 4–5. A (speculated) transformation from the proposed wurtzite-type FeS may also form these phases. O. Marcasite after pyrrhotite, see studies by MUROWCHICK (1992), FLEET (1978). P. Pyrite formed by sulfidation of pyrrhotite, see YUND and HALL (1970) for solid state kinetic study. This reaction is rapid above 573 K. Q. Troilite-hexagonal pyrrhotite reversible phase transition, see KRUSE (1992), KING and PREWITT (1982), HORWOOD *et al.* (1976) and PUTNIS (1974) for further details on intermediate structures and transition mechanisms.

observation (SCHOONEN and BARNES, 1991c) that the conversion rate of mackinawite to hexagonal pyrrhotite is relatively slow in alkaline solutions at elevated temperatures (453–473 K) when compared to the conversion rate in acidic and neutral solutions. The rate of the solid-state transformation

of mackinawite to pyrrhotite has been demonstrated to be slow below 530K (LENNIE *et al.*, 1995a) and, because it is a solid state transformation, unlikely to be affected by pH. Instead, we suggest that direct nucleation of hexagonal pyrrhotite from solution is enhanced at elevated tempera-

tures under acidic conditions, competing with formation of mackinawite. In addition, under acid conditions, dissolution of mackinawite will be more rapid than that of pyrrhotite allowing pyrrhotite to concentrate relative to mackinawite in acid solutions.

Sulfidation of iron 'monosulfides' forming iron disulfides

The formation of pyrite and marcasite in sedimentary and hydrothermal systems provides an important control on Fe and S in the environment. It has been proposed that at temperatures below 523 K or so, the direct nucleation of iron disulfides from solution is extremely slow compared to formation as a result of sulfidation of the 'monosulfide' precursors (SCHOONEN and BARNES, 1991a,b,c).

Sulfidation of amorphous FeS by H₂S or HS proceeds at an insignificantly slow rate at 338 K (SCHOONEN and BARNES, 1991b). However, at or above 373 K, sulfidation by H₂S proceeds at measurable rates (DROBNER *et al.*, 1990; SCHOONEN and BARNES, 1991c; TAYLOR *et al.*, 1979a,b); reduction of H ions forming H₂ balances the redox requirements of this reaction. Sulfidation of iron 'monosulfides' proceeds rapidly in the presence of S as polysulfide and/or zerovalent S (RICKARD, 1975).

It is expected that mackinawite, being the predominant 'FeS' phase formed in reducing solutions, would provide facile topotactic sites for pyrite or marcasite nucleation. Because mackinawite is so easily oxidised to greigite, greigite may also form a suitable precursor for pyrite or marcasite nucleation. To form a small pyrite (or marcasite) nucleus of unit-cell dimensions for further crystal growth from the surface would require relatively few bonds of the greigite structure to be broken and reformed. Although the role of the crystal surface is thought to be of importance in these sulfidation reactions, the site(s) of nucleation of pyrite or marcasite crystallites on the iron monosulfide precursor remains unknown. Further progress in elucidating mechanisms of S addition to Fe monosulfides will depend on carefully designed surface science studies of these reactions.

CONCLUDING REMARKS

Experimental data reported here can be combined with other literature data to obtain a summary of known low temperature phase relations in the iron-sulfur system. This summary is presented in Fig. 7, with footnotes referencing the literature sources of the relevant information.

The sequence of sulfidation of iron 'monosulfides' is seen to follow two main paths, the first being that of sulfidation of iron sulfides with ccp S sub-lattices, leading to formation of pyrite and marcasite (the Cubic FeS-mackinawite-greigite-marcasite/pyrite sequence). The second is that of sulfidation of pyrrhotite, again leading to pyrite, marcasite.

For iron sulfides FeS_{1+x}, with $x < 0.33$, the thermodynamic driving force is in the direction of formation of hcp S sub-lattices from ccp S sub-lattices, i.e. mackinawite to hexagonal pyrrhotite, greigite to ?hexagonal pyrrhotite (see Fig. 1). The predominant sulfidation sequence occurring in nature at low temperatures (<523 K), however, is the first sequence shown in Fig. 7. The abundant nucleation of pyrite or marcasite in sedimentary systems thus depends on metastable precursors which, in turn, are prevented by kinetic factors from transforming to stable pyrrhotites. It is noted that additional formation pathways resulting from dissolution or oxidation of iron sulfides, with subsequent precipitation of iron sulfide phases, are not addressed in Fig. 7.

This figure serves to show that the complex phase relations in the low temperature iron-sulfur system are now being clarified although further work is still required to clearly establish the relationship of smythite to other phases in this system. Our study demonstrates again the importance of metastable phases in the iron-sulfur system. Further studies are now required to clarify the role of surface structure and reactivity in formation and transformation of these phases.

Acknowledgements—The support of the Natural Environment Research Council is acknowledged. Thanks are due to Drs. J. M. Charnock, K.E.R. England, J. F. W. Mosselmans and P. F. Schofield for help with various aspects of the experimental work. Discussions with Professors George Helz and Jack Tossell were of great value in developing this work.

This paper is dedicated to the memory of Roger Burns who inspired and encouraged the efforts of both authors in studies of the crystal chemistry and geochemistry of iron sulfides.

REFERENCES

- BERNER R. A. (1964) Iron sulfides formed from aqueous solution at low temperatures and atmospheric pressure. *J. Geol.* **72**, 293–306.
- BINSTEAD N., CAMPBELL J. W., GURMAN S. J. and STEPHENSON P. C. (1991) 'SERC Daresbury Laboratory EXCURV92 program'.
- BONEV I. K., KHRISCHEV KH. G., NEIKOV H. N. and GEORGIEV V. M. (1989) Mackinawite and greigite in iron sulphide concretions from Black Sea sediments. *C. R. Acad. Bulg. Sci.* **42**, 2, 97–100.

- BROWN G. E. JR., CALAS G., WAYCHUNAS G. A. and PETIAU J. (1988) X-ray absorption spectroscopy and its applications in mineralogy and geochemistry. In *Spectroscopic Methods in Mineralogy and Geology* (ed. F. C. HAWTHORNE) *Rev. in Mineral.* **18**, pp. 431–512. Mineralogical Society of America.
- BUCKLEY A. N. and WOODS R. (1985) X-ray photoelectron spectroscopy of oxidised pyrrhotite surfaces. I. Exposure to air. *Appl. Surf. Sci.* **22/23**, 280–287.
- BUCKLEY A. N. and WOODS R. (1987) The surface oxidation of pyrite. *Appl. Surf. Sci.* **27**, 437–452.
- BURDETT J. K. (1980) How some simple solids hold together. The use of the fragment formalism in crystal chemistry. *J. Am. Chem. Soc.* **102**, 450–460.
- CALAS G., BASSETT W. A., PETIAU J., STEINBERG D., TCHOUBAR D. and ZARKA A. (1984) Mineralogical applications of synchrotron radiation. *Phys. Chem. Miner.* **11**, 17–36.
- CALAS G., MANCEAU A., COMBES J. M. and FARGES F. (1990) Application of EXAFS in mineralogy. In *Absorption spectroscopy in mineralogy* (eds. A. MOTTANA and F. BURRAGETO) pp. 172–205. Elsevier, Amsterdam.
- CHASE M. W., JR., DAVIES C. A., DOWNEY J. R., JR., FRURIP D. J., McDONALD R. A. and SYVERUD A. N. (1985) JANAF thermochemical tables. *J. Phys. Chem. Ref. Data* **14**, 1198–1199.
- DAIKUN G. P., GREAVES G. N., HASNAIN S. S. and QUINN P. D. (1984) Daresbury Laboratory Technical Memorandum, DL/SCI/TM38.
- DAVISON W. (1991) The solubility of iron sulphides in synthetic and natural waters at ambient temperature. *Aquatic Sciences* **53/4**, 309–329.
- DE MEDICIS R. (1970a) Une nouvelle forme de sulfure de fer. *Rev. Chim. Miner.* **7**, 723–728.
- DE MEDICIS R. (1970b) Cubic FeS, a metastable iron sulfide. *Science* **170**, 1191–1192.
- DROBNER E., HUBER H., WACHTERHAUSER G., ROSE D. and STRETTNER K. O. (1990) Pyrite formation linked with hydrogen evolution under anaerobic conditions. *Nature* **346**, 6286, 742–744.
- FLEET M. E. (1970) Structural aspects of the marcasite-pyrite transformation. *Canad. Mineral.* **10**, 225–231.
- FLEET M. E. (1978) The pyrrhotite-marcasite transformation. *Canad. Mineral.* **16**, 31–35.
- FURUSETH S. and KJESKSHUS A. (1965) On the properties of α -MnS and MnS₂. *Acta Chem. Scand.* **19**, 1405–1410.
- GRØNVOLD F. and STØLEN S. (1992) Thermodynamics of iron sulfides II. Heat capacity and thermodynamic properties of FeS and of Fe_{0.875}S at temperatures from 298.15 K to 1000 K, of Fe_{0.98}S from 298.15 K to 800 K, and of Fe_{0.89}S from 298.15 K to about 650 K. Thermodynamics of formation. *J. Chem. Thermodyn.* **24**, 913–936.
- GURMAN S. J., BINSTED N. and ROSS I. (1984) A rapid, exact curved-wave theory for EXAFS calculations. *J. Phys. C* **17**, 143–151.
- GURMAN S. J., BINSTED N. and ROSS I. (1986) A rapid, exact curved-wave theory for EXAFS calculations: II. The multiple-scattering contributions. *J. Phys. C* **19**, 1845–1861.
- HORWOOD J. L., TOWNSEND M. G. and WEBSTER A. H. (1976) Magnetic susceptibility of single-crystal Fe_{1-x}S. *J. Sol. St. Chem.* **17**, 35–42.
- HYLAND M. H. and BANCROFT G. M. (1989) An XPS study of gold deposition at low temperatures on sulphide minerals: Reducing agents. *Geochim. Cosmochim. Acta* **53**, 367–372.
- JOYNER R. W., MARTIN K. J. and MEEHAN P. (1987) Some applications of statistical tests in analysis of EXAFS and SEXAFS data. *J. Phys. Chem.* **20**, 4005–4012.
- KING H. E. JR. and PREWITT C. T. (1982) High-pressure and high-temperature polymorphism of iron sulfide (FeS) *Acta Cryst. B* **38**, 1877–1887.
- KISSIN S. A. and SCOTT S. D. (1982) Phase relations involving pyrrhotite below 350°C. *Econ. Geol.* **77**, 1739–1754.
- KJESKSHUS, A, NICHOLSON, D. G. and MUKHERJEE, A. D. (1972) On the bonding in tetragonal FeS. *Acta Chem. Scand.* **26**, 1105–1110.
- KRUSE O. (1992) Phase transitions and kinetics in natural FeS measured by X-ray diffraction and Mössbauer spectroscopy at elevated temperatures. *Amer. Mineral.* **77**, 391–398.
- LEE P. A. and PENDRY J. B. (1975) Theory of the extended X-ray absorption fine structure. *Phys. Rev. B* **11**, 2795–2811.
- LENNIE A. R. (1994) Aspects of relations between metastable and stable phases in the iron-sulphur system. Unpublished PhD thesis, University of Manchester.
- LENNIE A. R. and VAUGHAN D. J. (1992) Kinetics of the marcasite-pyrite transformation: An infrared spectroscopic study. *Amer. Mineral.* **77**, 1166–1171.
- LENNIE A. R., ENGLAND K. E. R. and VAUGHAN D. J. (1995a) Transformation of synthetic mackinawite to hexagonal pyrrhotite: a kinetic study. *Amer. Mineral.* **80**, 960–967.
- LENNIE A. R., REDFERN S. A. T., SCHOFIELD P. F. and VAUGHAN D. J. (1995b) Synthesis and Rietveld crystal structure refinement of mackinawite, tetragonal FeS. *Min. Mag.* **59**, 677–683.
- MCINTYRE N. S. and ZETARUK D. G. (1977) X-ray photoelectron spectroscopic studies of iron oxides. *Anal. Chem.* **49**, 1521–1529.
- MUROWCHICK J. B. (1992) Marcasite inversion and the petrographic determination of pyrite ancestry. *Econ. Geol.* **87**, 1141–1452.
- MUROWCHICK J. B. and BARNES H. L. (1986a) Formation of Cubic FeS. *Amer. Mineral.* **71**, 1243–1246.
- MUROWCHICK J. B. and BARNES H. L. (1986b) Marcasite precipitation from hydrothermal solutions. *Geochim. Cosmochim. Acta* **50**, 2615–2629.
- PARISE, J. B. and SCHOONEN, M. A. A. (1990) An extended X-ray absorption fine structure (EXAFS) spectrographic study of amorphous FeS. *Geol. Soc. America Abst. Prog.* **22**, A293.
- PEARSON W. B. (1962) Relative atomic size in semiconductor chemistry. *J. Phys. Chem. Solids* **23**, 103–108.
- POWER L. F. and FINE H. A. (1976) The iron-sulfur system. I. The structure and physical properties of the compounds of the low temperature phase fields. *Miner. Sci. Eng.* **8**, 106–128.
- PRAIT A. R., MUIR I. J. and NESBITT H. W. (1994) X-ray photoelectron and Auger electron spectroscopic studies of pyrrhotite and mechanism of air oxidation. *Geochim. Cosmochim. Acta* **58**, 827–841.
- PUTNIS A. (1974) Electron-optical observations on the α -transformation in troilite. *Science* **186**, 439–440.
- RICKARD D. T. (1975) Kinetics and mechanism of pyrite formation at low temperatures. *Amer. J. Sci.* **275**, 636–652.
- RICKARD D. T. (1989) Experimental concentration time curves for the iron (II) sulfide precipitation process in

- aqueous solution and their interpretation. *Chem. Geol.* **78**, 315–324.
- SCHOONEN M. A. A. and BARNES H. L. (1991a) Reactions forming pyrite and marcasite from solution: I. Nucleation of FeS₂ below 100°C. *Geochim. Cosmochim. Acta* **55**, 1495–1504.
- SCHOONEN M. A. A. and BARNES H. L. (1991b) Reactions forming pyrite and marcasite from solution: II. Via FeS precursors below 100°C. *Geochim. Cosmochim. Acta* **55**, 1505–1514.
- SCHOONEN M. A. A. and BARNES H. L. (1991c) Mechanisms of pyrite and marcasite formation from solution: III. Hydrothermal processes. *Geochim. Cosmochim. Acta* **55**, 3491–3504.
- SHIRLEY D. A. (1972) High-resolution X-ray photoemission spectrum of the valence bands of gold. *Phys. Rev. B* **5**, 4709–4714.
- SHOESMITH D. W., TAYLOR P., BAILEY M. G. and OWEN D. G. (1980) The formation of ferrous monosulfide polymorphs during the corrosion of iron by aqueous hydrogen sulfide at 21°C. *J. Electrochem. Soc.* **127**, 1007–1015.
- TAKENO S., ZOKA H. and NIHARA T. (1970) Metastable cubic iron sulfide -with special reference to mackinawite. *Amer. Mineral.* **55**, 1639–1649.
- TAYLOR P. (1980) The stereochemistry of iron sulfides—a structural rationale for the crystallisation of some metastable phases from aqueous solution. *Amer. Mineral.* **65**, 1026–1030.
- TAYLOR P., RUMMERY T. E. and OWEN D. G. (1979a) Reactions of iron monosulphide solids with aqueous hydrogen sulphide up to 160°C. *J. Inorg. Nucl. Chem.* **41**, 1683–1687.
- TAYLOR P., RUMMERY T. E. and OWEN D. G. (1979b) On the conversion of mackinawite to greigite. *J. Inorg. Nucl. Chem.* **41**, 595–596.
- TOSSELL J. A. and VAUGHAN D. J. (1992) *Theoretical geochemistry: applications of quantum mechanics in the earth and mineral sciences*. Oxford University Press.
- TOSSELL J. A., VAUGHAN D. J. and BURDETT J. K. (1981) Pyrite, marcasite, and arsenopyrite type minerals: crystal chemical and structural principles. *Phys. Chem. Minerals* **7**, 177–184.
- VAUGHAN D. J. and CRAIG J. R. (1978) *Mineral chemistry of metal sulfides*. Cambridge University Press.
- VAUGHAN D. J. and LENNIE A. R. (1991) The iron sulphide minerals: their chemistry and role in nature. *Sci. Prog.* **75**, 371–388.
- WARD J. C. (1970) The structure and properties of some iron sulfides. *Rev. Pure Appl. Chem.* **20**, 175–206.
- WAYCHUNAS G. A. and BROWN G. E. JR. (1984) Applications of EXAFS and XANES spectroscopy to problems in mineralogy and geochemistry. In *EXAFS and Near Edge Structure III*. (ed. K. O. HODGSON), Springer Proc. Phys. **2**, 336–342. Springer.
- WELZ D. and ROSENBERG M. (1987) Electronic band structure of tetrahedral iron sulphides. *J. Phys. C* **20**, 3911–3924.
- WERTHEIM G. K. and BUCHANAN D. N. E. (1977) Core-electron line shapes in x-ray photoemission spectra from semimetals and semiconductors. *Phys. Rev. B* **16**, 2613–2617.
- YUND R. A. and HALL H. T. (1970) Kinetics and mechanism of pyrite exsolution from pyrrhotite. *J. Petrol.* **11**, 381–404.

